J Mater Sci (2011) 46:1571–1580
DOI 10.1007/s10853-010-4964-8

Preparation and properties of hollow silica tubes/cyanate ester hybrids for high-frequency copper-clad laminates

Dongxian Zhuo · Aijuan Gu · Guozheng Liang · Jiang-tao Hu · Li Yuan

Received: 8 May 2010 / Accepted: 29 September 2010 / Published online: 20 October 2010

Abstract A novel kind of hollow silica tube (HST)/cyanate ester (CE) hybrid with high thermal, mechanical, and dielectric properties for high-frequency copper-clad laminates (CCLs) was successfully developed. The curing behavior, the chemical structure of cured networks, and typical performance of HST/CE hybrids were systematically evaluated and compared with that of CE resin. Results disclose that the addition of HST into CE resin can obviously not only catalyze the curing of CE, but also change the chemical structure of resultant networks, and thus result in significantly improved mechanical, thermal, and dielectric properties. The hybrid with 0.7 wt% HST exhibits very good toughness; its impact strength is about 2.2 times of that of CE resin. The outstanding integrated properties show that HST/CE hybrids can be used as high performance structural and functional materials, especially high-frequency CCLs.

Introduction

With the rapid worldwide development of electrical science and technology, high performance copper-clad laminates (CCLs) which can translate information by high frequency and high speed have gained increasing demands from the whole IT and the related industry [1]. CCL is a kind of composites made of the resin matrix, reinforced fibers, and coppers. From the Principles of Composites, it is known that the matrix resin plays a determinate role in the performance of a composite, and so high-frequency CCLs must be fabricated using high performance matrices with integrated properties, especially outstanding dielectric, mechanical, and thermal properties as well as desirable processing [2–4].

Cyanate ester (CE) resins have outstanding integrated properties, such as excellent dielectric property, thermal resistance as well as good processing characteristics etc., and so CE resins have been regarded as the candidate with the greatest competition to fabricate advanced functional/structural materials for many cutting edge fields including microelectronic, aerospace, and transportation in the twenty first-century [5, 6]. However, like most thermosetting resins, the major drawback of CE resins is the inherent brittleness, a factor that often restricts structural applications. In addition, CE needs to be cured at very high temperatures. High curing temperature not only causes high energy consumption, and more importantly, the resultant cured resins tend to have higher stress concentration and internal defects, and thereby declining the integrated properties of resultant materials. To date, many methods have been developed to improve the two problems; however, they generally are proved to be difficult in overcoming the two disadvantages without sacrificing the excellent properties (especially dielectric and thermal properties) of the original CE resin.

"Inorganic-filler toughening" has been an important method for toughening polymers because it has the possibility for obtaining toughness and rigidity at the same time as well as favorable performance-cost ratio [7, 8]. Until now, some inorganic fillers, such as $CaCO_3$, ZrO_2 and silica with various geometries, etc., have been used to toughen thermosetting resins. Results reveal that the

D. Zhuo · A. Gu (✉) · G. Liang (✉) · J. Hu · L. Yuan
Department of Materials Science and Engineering, College of Chemistry, Chemical Engineering and Materials Science, Soochow University, Suzhou 215123, China
e-mail: ajgu@suda.edu.cn

G. Liang
e-mail: lgzheng@suda.edu.cn

toughening effect is greatly dependent on the size and content of inorganic fillers, as well as the interfacial adhesion between organic resin and inorganic fillers [9–12]. At present, lots of investigations have been focused on toughening thermoplastics [13–16], and some toughened thermoplastics have been successfully utilized in applications. Compared with these attractive progresses in thermoplastics, the process of toughening thermosetting resins by inorganic fillers still has a long way to go.

Since 1990, various nano inorganic tubes have considerably attracted the interests of scientists and engineers because of their great potentialities in many applications, and lots of attempts have been made to modify thermosetting resins. Many researches reported that the addition of carbon nanotubes into thermosetting resins can improve the toughness of these resins; however, carbon nanotubes need to be surface treated to improve their interaction with organic resins. Moreover, they tend to decline the dielectric properties of original resins because of their high dielectric constant and loss. Note that generally the maximum improvement in toughness by the addition of nanotubes is in the range of 60–70%, indicating that nano size may not be the suitable size for getting the optimum toughening effect [17, 18]. Therefore, a suitable variety of inorganic tubes with optimal, convenient size and good interaction with organic resin as well as preferred dielectric and thermal properties is a guarantee for developing high performance resins for high-frequency CCLs.

In this article, hollow silica tube (HST) with a diameter of 300–500 nm and a length of about 50–60 μm was synthesized by an organic templating method, and used to modify CE resin. The synthesized HST has abundant hydroxyl groups, enabling a chemical reaction with CE, and thus good interaction between inorganic and organic phases [19]. The effect of the content of HST on the integrated properties of CE resin including curing behavior of CE, and performance of cured resin are systematically evaluated. The aim of this article is not only to develop a new kind of high performance resins for high-frequency CCLs, but also to provide a new example in developing the toughening mechanism of thermosetting resins.

Experimental

Materials

2,2′-Bis (4-cyanatophenyl) isopropylidene (CE) was bought from Shangyu Chemical Ltd of Zhejiang in China. D, L-Tartaric acid, tetraethyl orthosilicate (TEOS), ammonia, and ethanol were commercial products with analytical grades and used without further purification.

Preparation of HST

HST was synthesized by hydrolyzing TEOS using D, L-tartaric acid as a template according to the literature [20]. A typical procedure for synthesizing HST: 0.73 g of TEOS was added into 5 mL of ethanol containing 0.02 g of D, L-tartaric acid and 0.06 g of distilled water, and the mixture solution was allowed to stand for 30 min. Subsequently, 2 mL of 28% aqueous NH_3 was added to the solution and allowed to stand for 30 min. The whole process described above was done at 25 °C. The product was washed with a large amount of water on a test sieve with 63-μm aperture to remove colloidal aggregates and HST with small aspect ratio, and then dried at 100 °C for 6 h under vacuum to remove the water.

Preparation of HST/CE hybrids

The hybrids were prepared using in situ polymerization followed by casting and multi-step thermal curing. Appropriate amounts of CE and HST were dispersed by a high-speed homogenizer at 150 °C for 2 h, and then the mixture was degassed to remove entrapped air at 150 °C in a vacuum oven. Subsequently, the mixture was cast into a mold for curing and postcuring via the procedures of 180 °C/2 h + 200 °C/2 h + 220 °C/2 h, and 240 °C/4 h. Finally, the hybrid was demolded and coded as HST*n*/CE hybrid, where n represents the weight loading of HST in the hybrids, taking values of 0.3, 0.7, 1.3, 2.0, and 3.0 wt%.

Preparation of cured CE resin

Appropriate amount of CE was heated to 150 °C with stirring, and maintained at that temperature for 2 h, and then the molten CE was put into a preheated mold followed by degassing at 150 °C for 2 h in a vacuum oven. Then, the mold was put into an oven for curing and postcuring per the procedures of 180 °C/2 h + 200 °C/2 h + 220 °C/2 h and 240 °C/4 h, and the resultant product is that of cured CE resin.

Measurements

The concentration of silanol hydroxyl groups in HST and colloidal aggregates was determined by titration [21]. In detail, HST or colloidal aggregates (2 g) with ethanol (25 mL) and 20 wt% sodium chloride solution (75 mL) were added into a beaker (200 mL). The suspension was fully stirred, and then some amounts of hydrochloric acid (0.1 mol/L) were slowly added into the beaker to adjust the pH value of the suspension solution (pH = 4). Then, the suspension was titrated by sodium hydroxide solution

(0.1 mol/L) until the pH value of the solution equals 9. The content of silanol hydroxyl groups (C_{Si-OH}) in HST or colloidal aggregates was calculated according to Eq. 1:

$$C_{Si-OH} = \frac{CV \times 10^{-3}}{m} \quad (1)$$

where C is the concentration of sodium hydroxide solution, which is 0.1 mol/L; V is the volume of consumed sodium hydroxide solution when the pH value of the solution increases from 4 to 9; and m is the mass of HST or colloidal aggregates.

Fourier Transform Infrared (FTIR) spectra were recorded between 400 and 4000 cm^{-1} with a resolution of 2 cm^{-1} on a Nicolet FTIR 5700 spectrometer (USA).

Differential Scanning Calorimeter (DSC) measurements were performed with a DSC 2010 (TA Instruments, USA) ranging from room temperature to 320 °C at a heating rate of 10 °C/min under a nitrogen atmosphere.

A Scanning Electron Microscope (Hitachi S-4700, Japan) coupled with energy disperse X-ray spectrometer (EDS) was employed to observe the morphology of samples. The resolution of the secondary electron image is 1.5 nm under 15 kV. All the samples should be dried at 100 °C for 6 h before test.

Dynamic Mechanical Analysis (DMA) was performed using TA DMA Q800 apparatus from TA Instruments (USA). A single cantilever clamping mode was used. DMA tests were carried out from room temperature to 320 °C with a heating rate of 3 °C/min at 1 Hz. The sample dimension was $(35 \pm 0.02) \times (13 \pm 0.02) \times (3 \pm 0.02)$ mm^3.

Thermogravimetric (TG) analyses were performed on a TA Instruments model SDTQ600 (USA) in the range from 25 to 800 °C under a nitrogen atmosphere with a flow rate of 100 mL/min and a heating rate of 20 °C/min.

The dielectric constant and loss were measured using a Broadband Dielectric Spectrometer (Novocontrol Concept 80 analyzer, Germany) at the frequency between 1 and 10^6 Hz. The sample dimension was $(25 \pm 0.02) \times (25 \pm 0.02) \times (3 \pm 0.02)$ mm^3.

The unnotched impact strength was tested according to GB/T2571-1995 using Charpy Impact Machine Tester (XCJ-L, China); at least five samples for each formulation were broken.

The flexural strength was measured according to GB/T2570-1995 using a electronic universal testing machine (RIGER-20, China) at a crosshead speed of 2 mm/min.

Transmission Electron Microscopy (TEM) was recorded on a Tecnai G220 (Japan) with a 200 kV accelerating voltage. The samples were prepared by mounting a drop of the micelle solution (0.05 mL) on a copper EM grid covered with a thin film of formvar.

Results and discussion

Characterization of HST

Figure 1 gives SEM and TEM images of HST, and it can be clearly seen that HST is hollow and polygonal-shaped tube with a diameter of 300–500 nm and a length of about 50–60 μm, and so the corresponding aspect ratio of HST is about 100–200. Alongside the tubes, there are still some small quantities of silica particles.

The chemical structure of synthesized HST was characterized by FTIR spectroscopy as shown in Fig. 2. There are three absorption bands at 3397, 1090, and 936 cm^{-1}, attributed to the absorptions of –OH, Si–O–Si, and Si–OH groups, respectively, reflecting that the organic template is removed completely and many silanol hydroxyl groups exist on the surface of HST. According to the result of titration, the concentration of silanol hydroxyl groups in HST is 0.44×10^{-3}mol/g, which is slightly less than that in colloidal aggregates (0.54×10^{-3}mol/g).

Effect of HST on the curing behavior of CE

Gel time is generally used to evaluate the curing behavior of a resin: a shorter gel time indicates a bigger curing reaction activity. Figure 3 depicts the influence of the content of HST on the gel time of CE at different temperatures. It can be observed that an addition of a small amount of HST can effectively decrease the gel time of CE (especially the gel time at relatively low temperature), indicating that the addition of HST can accelerate the gelation of CE, which may be attributed to the presence of silanol hydroxyl groups on the surface of HST.

In order to further confirm the effect of HST on the curing of CE, comparative DSC analyses of HST/CE and CE were carried out, and corresponding curves are depicted in Fig. 4. It can be seen that either CE or HST/CE has one exothermic peak, but the width and intensity of these peaks are obviously different. Specifically, the whole peak of HST/CE significantly shifts toward a lower temperature range than that of neat CE, demonstrating that the whole curing process of CE is pronouncedly accelerated by the addition of a small amount of HST loading; however, with continuously increasing content of HST (>2.0 wt%), the addition of HST does not significantly affect the peak temperature because of the steric effect of HST during the curing reaction of CE [22]. In addition, hybrids exhibit a broader exothermic peak as the amount of HST increases because of a possible heat of reaction caused by the formation of the imidocarbonate intermediate [23–25].

Interestingly, with careful observation, it can be found that the intensity of exothermic peak of HST/CE is much less than that of CE, indicating that the incorporation of

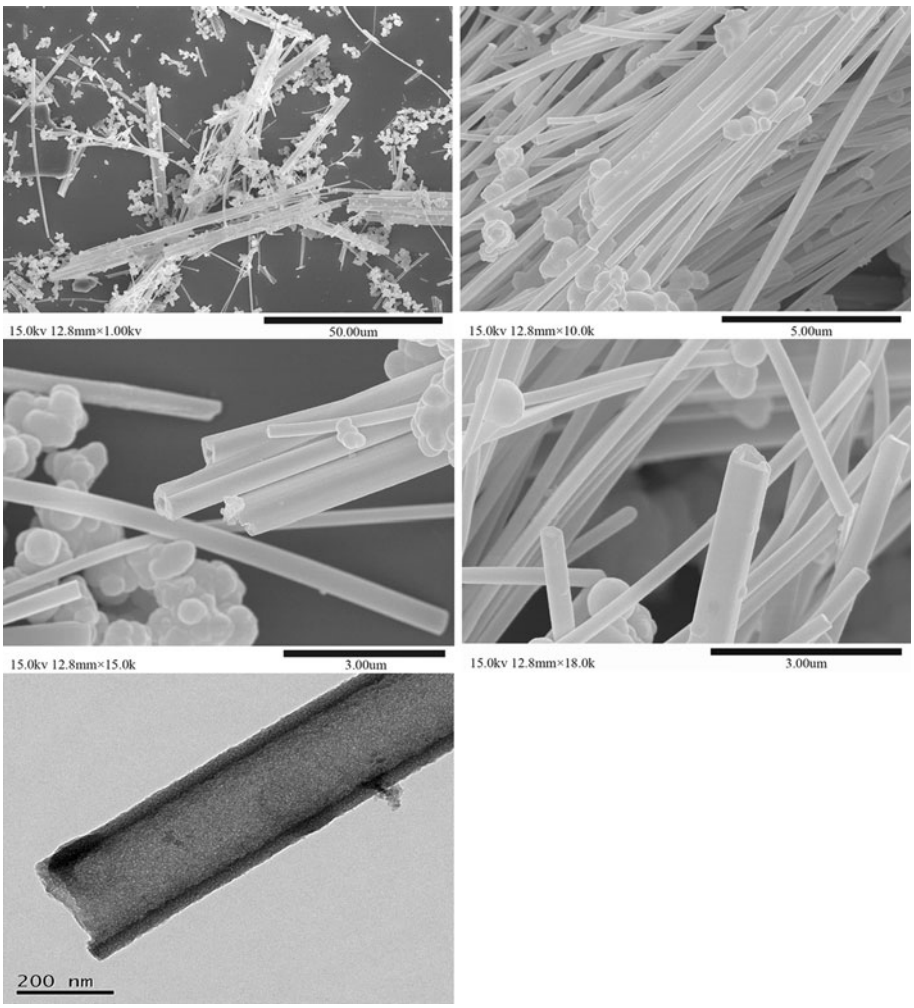

Fig. 1 SEM and TEM images of HST

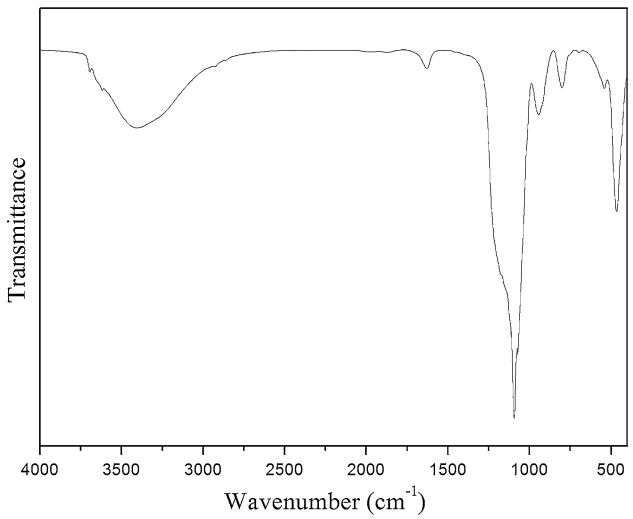

Fig. 2 FTIR spectrum of HST

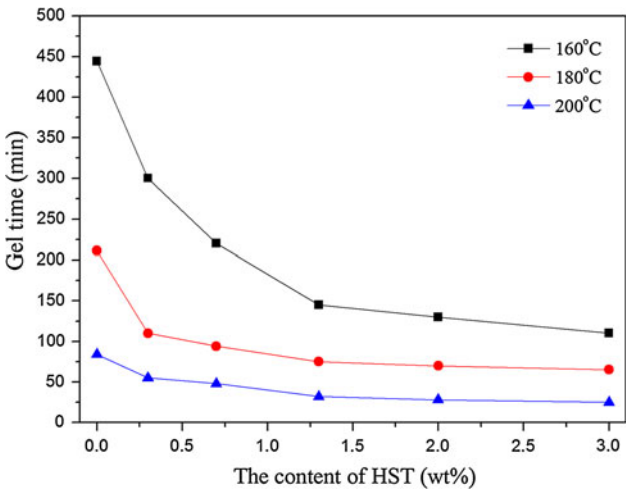

Fig. 3 Dependence of gel time on temperature of CE and various HST/CE systems

HST into CE significantly makes the whole curing reaction change from a strong reaction to a moderate one; therefore, the curing reaction of HST/CE system avoids heat accumulation and thermal explosion, controlling of which is thus easily achieved. It is a very attractive feature for fabricating materials, especially those with big thickness.

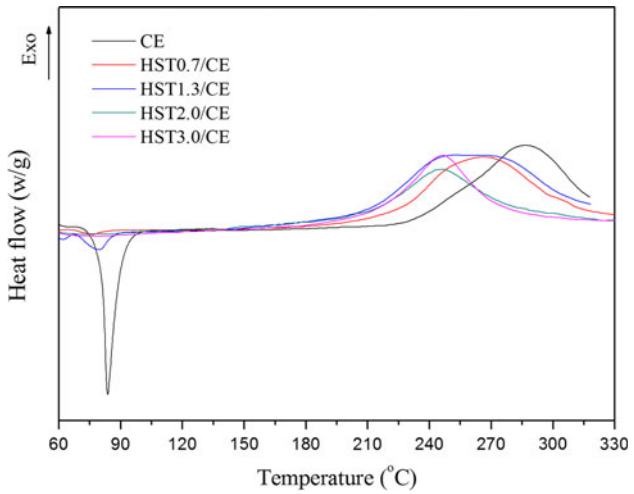

Fig. 4 DSC curves of neat CE and HST/CE hybrids with various contents of HST

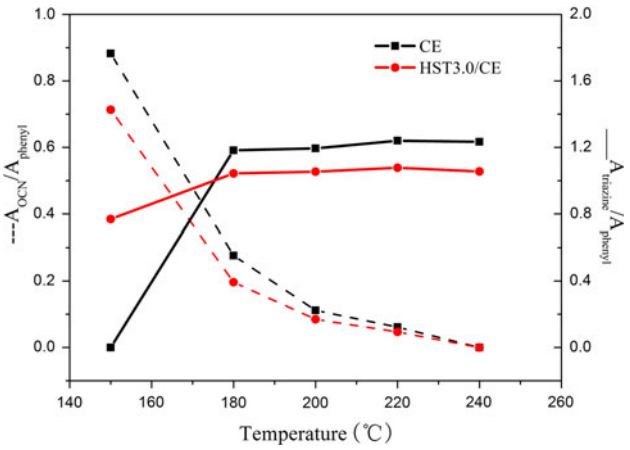

Fig. 6 Relative IR absorption intensities of –OCN and triazine groups of CE and HST3.0/CE after curing at various stages (the *X* axis is the final curing temperature of each curing stage)

Chemical structures of cured CE resin and HST/CE hybrids

In order to detect the change in chemical structure during the curing process, the whole curing procedure is divided into five stages, and the samples after cured at various stages were prepared for analyses.

Figure 5 gives the FTIR spectra of CE and HST3.0/CE after curing at various stages. With the progress of curing process, the intensities of the absorption bands assigned to the stretching vibration of –OCN groups (2274 and 2237 cm^{-1}) decrease gradually, while those of the absorption bands attributing to the absorptions of triazine rings at 1563 and 1369 cm^{-1} drastically increase. These data are easy to be understood because the main curing reaction of CE is the cyclotrimerization of the –OCN groups to form triazine rings [26].

In order to quantitatively compare the reactivities of CE and HST3.0/CE, the relative intensities of –OCN group and triazine ring with respect to that of symmetric vibration absorbance of phenyl ring (A_{Phenyl}, at 1500 cm^{-1}) are calculated, and the results are depicted in Fig. 6. It can be seen that after curing at any stage, the relative intensity of –OCN for CE is greater than that for HST3.0/CE, suggesting that CE has slower reactivity than HST/CE, which further proves that HST has catalyzing effect on the curing of CE. Hence, it is expected that HST3.0/CE has larger conversion of triazine ring than CE, but this expectation is not true except for the samples cured at 150 °C. Specifically, after curing at 150 °C, almost no triazine ring forms in the CE sample, while some triazine rings exist in HST3.0/CE because of the catalyzing role of HST. However, after curing at 180 °C or higher temperature, the yield of triazine ring in CE sample is inversely bigger than that in HST3.0/CE, and thereby reflecting that –OCN groups in HST3.0/CE not only produce triazine ring, but also form some other chemical structure. In conclusion, cured CE resin and HST3.0/CE have different crosslinking networks, which can also be proven by the presence of new absorption bands as shown in Fig. 5.

Compared with FTIR spectra of CE, there are some new absorptions in the FTIR spectra of HST3.0/CE. First, the peak at about 1640 cm^{-1} maybe due to the formation of

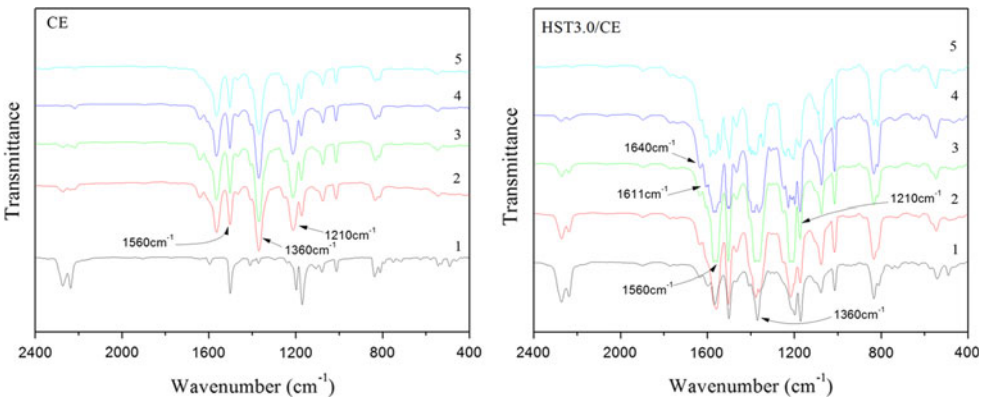

Fig. 5 FTIR spectra of CE and HST3.0/CE cured per different procedures: (*1*) 150 °C/2 h, (*2*) 150 °C/2 h + 180 °C/2 h, (*3*)150 °C/2 h + 180 °C/ 2 h + 200 °C/2 h, (*4*) 150 °C/ 2 h + 180 °C/2 h + 200 °C/ 2 h + 220 °C/2 h, (*5*) 150 °C/ 2 h + 180 °C/2 h + 200 °C/ 2 h +220 °C/2 h +240 °C/4 h

(≡SiO)C=NH group by silanol–cyanate reaction [27], which is supported by results of DSC. Second, a new N–H in-plane bending peak appearing at 1560 cm^{-1} can be attributed to the formation of iminocarbonate structure [28]. Third, in the case of HST/CE after curing at 200 °C or even higher temperatures, a new absorption at 1611 cm^{-1} attributed to the formation of (≡SiO)C=N–C=NH appears [29]. Fourth, simultaneously, three broadening bands at about 1210, 1369, and 1563 cm^{-1}, corresponding to the stretching vibrations of C–O–C, C–N, and C=N, respectively, are likely related with further reactions at the iminocarbonate functions in the hybrids, which indirectly prove the silanol–cyanate reaction (Scheme 1).

Altogether, the addition of HST into CE significantly changes the chemical structure of the resultant network.

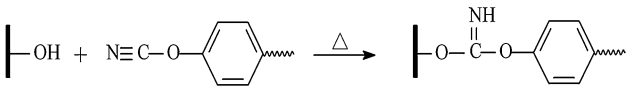

Scheme 1 Proposed reaction between Si–OH and –OCN groups

That is, the reaction between Si–OH and –OCN introduces –OCN on the surface of HST, and guarantees the good dispersion of HST in the CE resin matrix which can be confirmed by the Si mapping results of the fracture surfaces of HST0.7/CE and HST3.0/CE hybrids by EDS analyses as shown in Fig. 7. It can be seen that bright dots corresponding to Si atoms homogeneously distribute in each picture, reflecting that HST is well dispersed in the resin matrix of HST/CE hybrids. Such changes in network structure will affect the macroscopic properties of HST/CE hybrids.

Mechanical properties of HST/CE hybrids

Mechanical properties are important properties of a resin matrix for advanced composites, especially those used as structural materials. Flexural property is usually used for evaluating the integrated mechanical properties of a material because the flexural loading is very complicated and may contain multi-type loadings such as tensile, shearing, and/or compressing loadings [30].

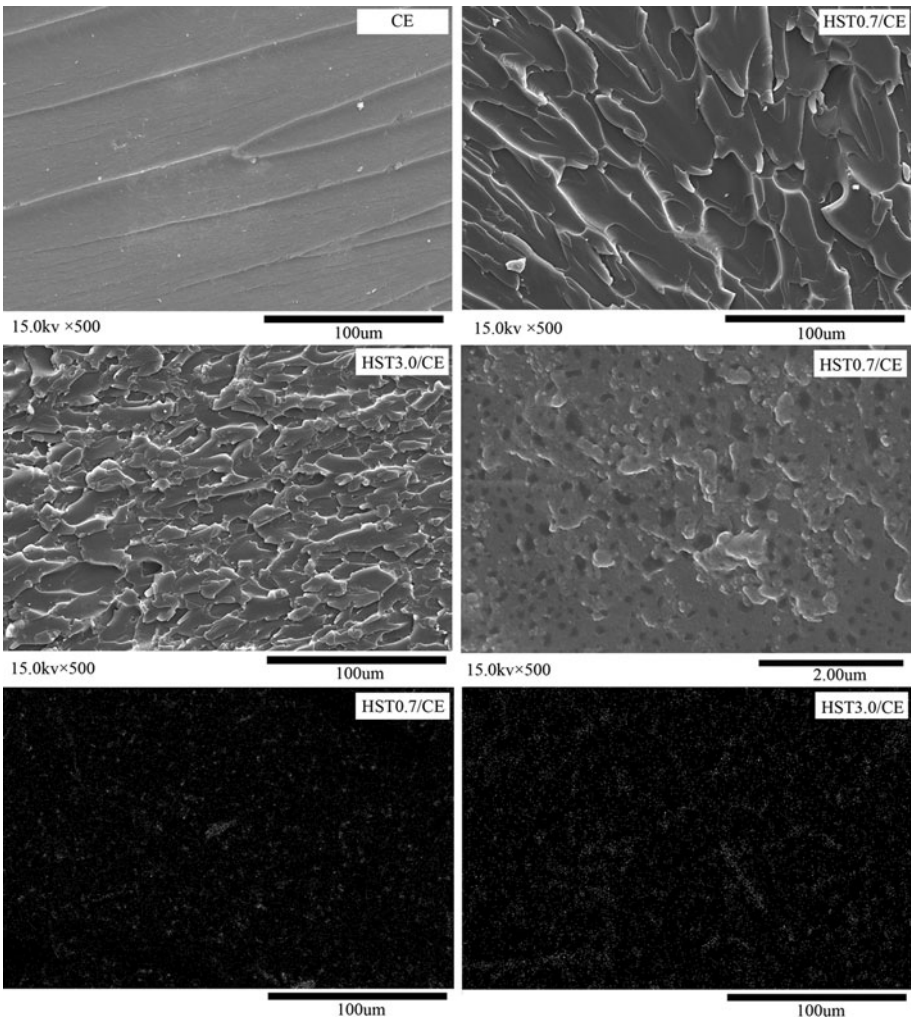

Fig. 7 SEM micrographs and Si mapping (EDS) of cured CE resin and HST/CE hybrids

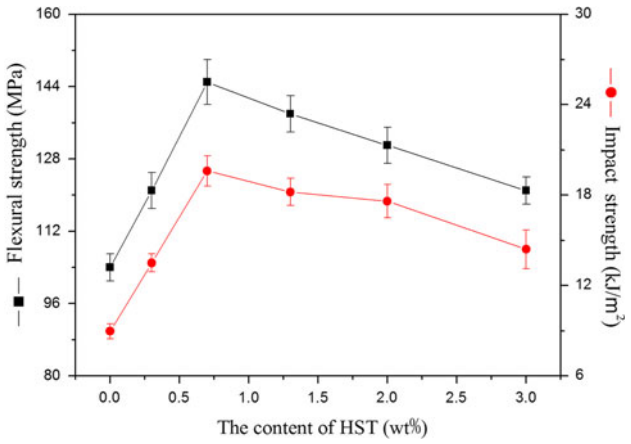

Fig. 8 Dependence of the content of HST on the flexural and impact strengths of cured HST/CE hybrids

The flexural strengths of cured HST/CE hybrids are presented in Fig. 8. All hybrids have higher flexural strengths than neat CE resin because of the reinforcement of rigid fillers, which comes from the desirable interfacial interaction between HST and CE resin matrix. On the other hand, the flexural strength of hybrids is greatly dependent on the content of HST, which initially increases with the increase of the content of HST, and then reaches the maximum value (145 MPa) at 0.7 wt% HST.

The reinforcement of nanoparticles to polymeric matrices possibly arises from the optimum particle network and efficient interfacial interaction between inorganic and organic phases (thus, good stress transfer) [31]. Such an optimum network is expected to form when the concentration of nanoparticles exceeds its critical threshold. For HST prepared herein, its aspect ratio is 100–200, so the corresponding percolation threshold is 0.35–0.74 wt% calculated by the method described in the literature [32]. The estimated threshold is consistent with the optimum content of HST for obtaining the maximum flexural strength.

On the other hand, the interfacial interaction will be contributing to the domain role in the reinforcing effect when the loadings of fillers are insufficient to form optimum particle networks [31]. As analyzed in the FTIR part, there are covalent bonds between HST and organic resin matrix; further evidence will be found in the shape of damping curve by DMA technique, and the morphologies of HST/CE hybrids by SEM technique. Detailed discussion will be taken up in the later part of this article.

The co-reaction between Si–OH and –OCN provides good chemical adhesion between HST and CE resin matrix. Meanwhile, as described above, HST are hollow with a diameter of 300–500 nm, and so it is possible for some CE molecules to enter the interiors of some amount of HST, triggering a physical interaction between HST and CE resin matrix. As shown in the fractured surfaces of cured HST0.7/CE and HST3.0/CE hybrids (Fig. 7), the failure of the HST/CE hybrids seldom takes place at the interface between HST and CE resin; moreover, it is difficult to find a whole HST on the fractured surface because of the formation of chemical and physical interactions between HST and CE resin matrix.

As thermosets are usually brittle, so toughening has been the main subject for thermosetting resins, which is generally evaluated by impact strength. From the impact strengths of cured CE resin and hybrids shown in Fig. 8, it can be seen that the dependence of impact strength on the content of HST is similar to that of flexural strength. Note that HST0.7/CE hybrid has the maximum impact strength which is about 2.2 times of the impact strength of CE resin. This increase is much more than would be expected with similar content of silica fillers, which is only 1.3–1.6 times of the impact strength of CE resin [24, 33, 34]. The increased toughness from CE resin to HST/CE hybrids can also be confirmed by observing their SEM micrographs of the fractured surfaces. The fracture surface of CE resin shows smooth ribbon structures, which is typical of brittle feature (Fig. 7), while HST0.7/CE hybrids has much rougher fractured surface.

Thermal properties of cured HST/CE hybrids

Thermal properties are generally characterized by glass transition temperature (T_g) and thermogravimetric behavior. The former indicates the movement capacity of molecular chains with the increase of temperature, reflecting the maximum application temperature of the resin, whereas the latter denotes the thermal stability of molecular chains.

T_g can be tested by a few methods, among which, however, the one by defining T_g as the peak (maximum) temperature in the tan δ–temperature plot from DMA measurement is proven to be the most effective [35]. Figure 9 gives overlay tan δ–temperature curves from DMA tests of cured CE resin and HST/CE hybrids. The shape of tan δ peak may be used as a convenient indicator of the morphology for multiphase materials [36]. It can be seen that CE resin and hybrids show completely different tan δ–temperature curves. Specifically, CE resin has a strong and sharp peak at about 293 °C, indicating that CE resin possess single-phase structure; while all hybrids exhibit a complex shape, consisting of a strong and sharp peak with a small shoulder at low temperature, which can be divided into one big peak appearing at 280–287 °C and one small peak appearing at 242–252 °C by the Gaussian fitting [37], reflecting that HST/CE hybrids have multi-phase structure, and thus two T_g values. In the case of CE resin, it cures thorough thermal cyclotrimerization to form triazine ring

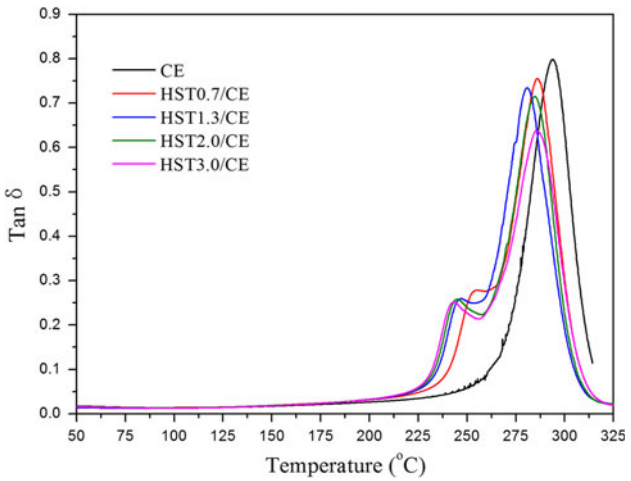

Fig. 9 Overlay curves of tan δ as a function of temperature for cured CE resin and HST/CE hybrids

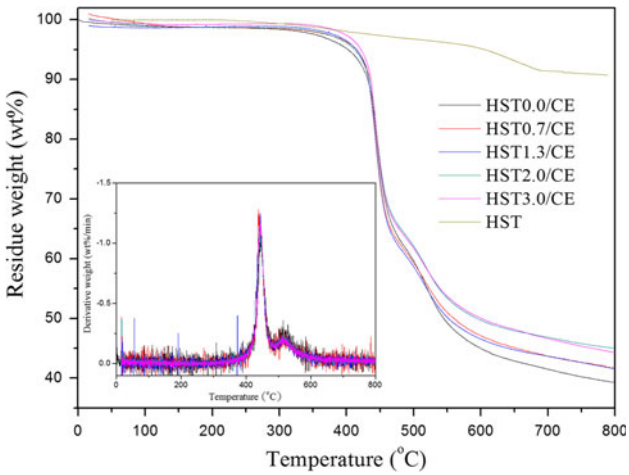

Fig. 10 TG and DTG curves of HST, cured CE resin and HST/CE hybrids

network. On the other hand, for HST/CE hybrids, besides the triazine ring network, the co-reaction between Si–OH and –OCN reduces the amount of triazines rings, and thus results in loose stacking of the macromolecules surrounding the solid particles and forming additional organic network [38, 39]. Therefore, their two T_g values represent above structures. This similar phenomenon also appeared in the damping spectra of other cyanate ester-based composites [24, 40].

With careful comparison, the transition temperatures corresponding to triazine ring-rich area of hybrids are slightly lower than that that of cured CE resin. This is because –OCN groups in the hybrids do not completely cyclotrimerize to form triazine rings, some of which co-react with Si–OH groups, and so the overall crosslinking degree of triazine rings is not as big as that for CE resin, resulting in slightly lower T_g value. On the other hand, many investigations have suggested that the relative heights in T_g dispersions are inversely proportional to the volume fraction of confined segments in the interface layer [41]; the markedly decreased intensities of two damping peaks of hybrids with increasing loading of HST imply that the increased HST loading increases the covalent bonding between HST and CE resin matrix.

The TG and DTG curves of cured CE resin and all hybrids are shown in Fig. 10. The corresponding initial degradation temperature (T_{di}) at which the weight loss of the sample reaches 5 wt%, the maximum degradation rate temperature (T_{max}), and char yield (Y_c) at 750 °C are summarized in Table 1. T_{di} is usually used to evaluate the thermal degradation and thermal stability of a material. The incorporation of HST efficiently improves the thermal stability, for example, the T_{di} of the hybrid with 0.7 wt% increases by 12 °C. Furthermore, it is worthy to note that Y_c values of all hybrids are significantly higher than that of

Table 1 Characteristic data from TG analyses of cured CE resin and HST/CE hybrids

Sample	T_{di} (°C)	T_{max} (°C)		Y_c at 750 °C (wt%)	
		T_{max1}	T_{max2}	Theoretical	Experimental
CE	402	443	517	–	40.2
HST0.7/CE	415	442	521	40.8	42.6
HST1.3/CE	416	443	519	41.4	42.7
HST2.0/CE	414	445	520	42.0	45.8
HST3.0/CE	421	445	520	42.9	45.3
HST	525	–	–	–	90.9

CE resin as well as theoretical values calculated by the "Mixture Rule." The reasons behind this phenomenon can be explained by the effect of HST on the curing network of the resultant hybrids as well as the hollow and fibrous structure of HST. The accelerated curing reactivity by Si–OH groups on the surface of HST allows an additional positive role on improving the thermal stability. On the other hand, the structure of HST has two influences on the thermal stability of HST/CE hybrids. First, it is well known that the thermal conductivity of air is extraordinary lower than that of a polymer, and so introducing hollow structure can effectively retard the heat entering into the internal resin matrix. Second, as described above, the interiors of some HST may be filled with CE molecules, and then the filled space weakens the effect of hollow structure on thermal conductivity; however, note that the filled HST can not only delay the thermal decomposition of organic resin, but also reduce the volatilizing rate of decomposition products. All these aspects combine together, and thus lead to the improved thermal stability of hybrids.

In addition, cured CE resin and all hybrids have similar DTG curves, suggesting that the incorporation of HST does

not change the thermal degradation mechanism of the resultant network.

Dielectric properties of cured HST/CE hybrids

A material with low dielectric constant and dissipation factor (loss) will reduce the delay time and loss of signal propagating. Hence, low dielectric constant and loss is the characterizing feature of materials for IT industry.

Figure 11 shows the frequency dependence of the dielectric constant of HST/CE at room temperature. All hybrids with low content of HST (<2.0 wt%) have similar excellent stability of dielectric constant on frequency as CE resin. When the content of HST is bigger than 2.0 wt%, the dielectric constant of hybrids is sensitive to the frequency (lower than 10^4 Hz); this becomes pronounced with increasing the content of HST.

With regard to the exact value of the dielectric constant of hybrids, this is also closely related with the content of HST. Because HST has much lower dielectric constant than CE resin, it is expected that HST/CE hybrids have lower dielectric constant than CE resin, and the more the content of HST is, the lower the dielectric constant is. However, this expectation is true only when the content of HST is lower than 0.7 wt%: the dielectric constant gradually increases with further increase of the content of HST. Besides the low dielectric constant of HST, this phenomenon can be interpreted by following reasonings. First, as discussed above, the addition of HST into CE resin changes the chemical structure of the resultant network. Triazine ring is the main structure of cured CE resin—the high degree of polar symmetry tends to balance the pull of electrons—resulting in short dipole moment and low energy storage in an electromagnetic field; these features are responsible for the lower dielectric constant of CE resin. On the other hand, in the case of HST/CE hybrids, especially those with high content of HST, additional products from the reaction between –Si–OH and –OCN not only increase the polarity, but also decline the degree of polar symmetry, leading to greater dielectric constant.

Second, dielectric properties of polymers depend on the orientation and relaxation of dipoles in the applied electric field, the process of dipole polarization is accompanied by the segmental movement of polymer chains, therefore, the dielectric properties are closely related to the interaction between inorganic and organic phases. Because HST has good interaction with CE resin matrix, the presence of HST tends to provide big restricting influence on the orientation and relaxation of dipoles in the applied electric field, thereby resulting in low dielectric constant.

When the filler loading is small, the second effect and the nature of low dielectric constant of HST play the dominate role, and so HST/CE hybrid has gradually decreased dielectric constant with increasing the content of HST. On the other hand, when the filler loading is high enough, the first reason becomes the dominate factor, so the corresponding hybrids show enlarged dielectric constant.

The dependences of dielectric loss on the frequency and content of HST of hybrids is depicted in Fig. 12. HST0.3/CE and HST0.7/CE hybrids show slightly better stability of dielectric loss on frequency than CE resin, while the former has almost equal dielectric loss as the latter. With increasing content of HST, the dielectric loss of hybrids gradually tends to be sensitive to the frequency (lower than 10^4 Hz), and this phenomenon becomes pronounced with further increased content of HST in hybrid.

Altogether, owing to the reduced dielectric constant as well as low and better stability of dielectric loss, HST/CE hybrids with suitable content of HST shows greater

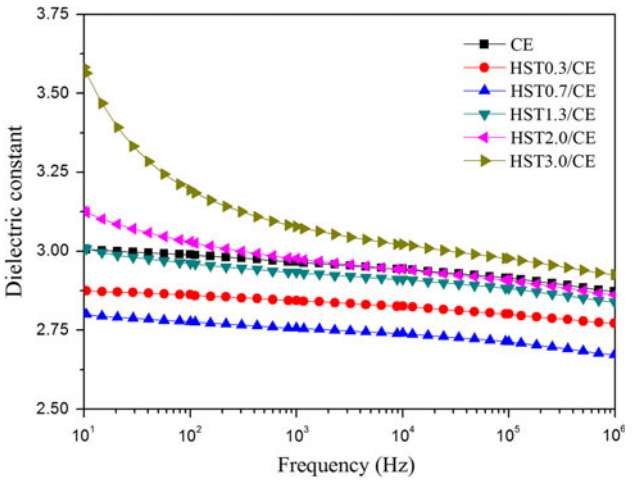

Fig. 11 Dependence of dielectric constant on frequency for cured CE resin and HST/CE hybrids

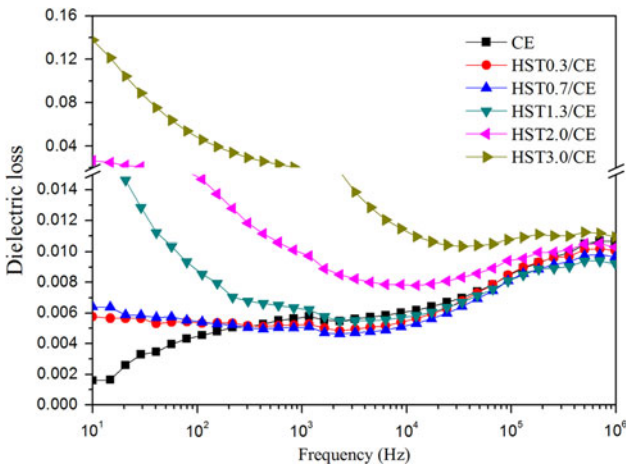

Fig. 12 Dependence of dielectric loss on frequency for cured CE resin and HST/CE hybrids

potentialities to meet the urgent need in dielectric properties of high-frequency CCLs, compared with original CE resin.

Conclusion

The addition of HST into CE resin matrix obviously not only catalyzes the curing reaction of CE, but also changes the chemical structure of resultant networks, thus resulting in significantly improved mechanical, thermal, and dielectric properties. The desirable mechanical and thermal properties of the hybrids can be attributed to the reinforcement of fillers and efficient interfacial interaction between HST and CE resin. The significantly improved dielectric properties of hybrids not only result from the restriction on chain segmental motions of polymer chains by HST, but also account for the variety in the chemistry of crosslinked network. The excellent integrated properties of HST/CE hybrids provide great potentialities to be used as structural and functional materials for many cutting-edge fields, especially high-frequency CCLs.

Acknowledgements The authors thank the Natural Science Foundation of China (20974076), China Postdoctoral Science Foundation (20080440165), "Qin Lan Project" (2008) and "Six Talent Peaks" (2008) of Jiangsu Province for financially supporting this project.

References

1. Chung WWC, Leung SWF (2005) Prod Plan Control 16:563
2. Duann YF, Chen BL, Tsai TH (2005) J Appl Polym Sci 95:1485
3. Lin HT, Lin CH, Hu YM, Su WC (2009) Polymer 50:5685
4. Takahashi A, Satsu Y, Nagai A, Umino M, Nakamura Y (2005) IEEE Trans Electron Packag Manuf 28:163
5. Fang T, Shimp DA (1995) Prog Polym Sci 20:61
6. Ganesan A, Muthusamy S (2008) J Polym Res 15:507
7. Mackay ME, Tuteja A, Duxbury PM, Hawker CJ, Horn BV, Guan ZB, Chen GH, Krishnan RS (2006) Science 311:1740
8. Vaia RA, Maguire JF (2007) Chem Mater 19:2736
9. Lu HB, Shen HB, Song ZL, Shing KS, Tao W, Nutt S (2005) Macromol Rapid Commun 26:1445
10. Zhu Y, Sun DX, Zheng H, Wei M, Zhang LM (2007) J Mater Sci 42:545. doi:10.1007/s10853-006-1066-8
11. Vendamme R, Onoue SY, Nako A, Kunitake T (2006) Nat Mater 5:494
12. Moniruzzaman M, Chattopadhyay J, Billups WE, Winey KI (2007) Nano Lett 7:1178
13. Zhang YH, Lu SG, Li YQ, Dang ZM, John HX, Fu SY, Li GT, Guo RR, Li LF (2005) Adv Mater 17:1056
14. Zhang YH, Li YQ, Li GT, Huang HT, Chan HLW, Walid AD, John HX, Li LF (2007) Chem Mater 19:1939
15. Fu SY, Zheng B (2008) Chem Mater 20:1090
16. Jiang LY, Leu CM, Wei KH (2002) Adv Mater 14:426
17. Yu N, Zhang ZH, He SY (2008) Mat Sci Eng A 494:380
18. Fang ZP, Wang JH, Gu AJ (2006) Polym Eng Sci 46:670
19. Liang KW, Li GZ, Toghiani H, Koo JH, Pittman CU (2006) Chem Mater 18:301
20. Fumiaki M, Sean AD, Jonathon PHC, Stephen M (1999) Chem Mater 11:3021
21. Krysztafkiewicz A, Rager B, Jesionowski T (1997) J Mater Sci 32:1333. doi:10.1023/A:1018564808810
22. Zeng MF, Sun XD, Wang Y, Zhang MZ, Shen YM, Wang BY, Qi CZ (2008) Polym Adv Technol 19:1664
23. Barton JM, Hamerton I, Jones JR (1993) Polym Int 31:95
24. Pan YZ, Xu Y, An L, Lu HB, Yang YL, Chen W, Nutt S (2008) Macromolecular 41:9245
25. Henry CYK, Dai J, Tan E, Liang WR (2006) J Appl Polym Sci 101:1775
26. Lin RH, Lu WH, Lin CW (2004) Polymer 45:4423
27. Iijima T, Katsurayama S, Fukuda W, Tomoi M (2000) J Appl Polym Sci 76:208
28. Choi J, Harcup J, Yee AF, Zhu Q, Laine RM (2001) J Am Chem Soc 123:11420
29. Lin CH (2004) Polymer 45:7911
30. Song HC (1985) Polymer composites, 1st edn. Beijing University of Aeronautics & Astronautics Press, Beijing
31. An L, Pan YZ, Shen XW, Lu HB, Yang YL (2008) J Mater Chem 18:4928
32. Garboczi EJ, Snyder KA, Douglas JF (1995) Phys Rev E 52:819
33. Wooster TJ, Abrol S, Hey JM, Macfarlane DR (2004) Compos Part A 35:75
34. Wooster TJ, Abrol S, Macfarlane DR (2005) Polymer 46:8011
35. Bussu G, Lazzeri A (2006) J Mater Sci 41:6072. doi:10.1007/s10853-006-0694-3
36. Matsuoka S (1992) Relaxation phenomena in polymers. Spring Verlag, Munich
37. Anthony SM, Granick S (2009) Langmuir 25:8152
38. Ree M, Yoon J, Heo K (2006) J Mater Chem 16:685
39. Li QX, Simon SL (2008) Macromolecules 41:1310
40. Han CF, Gu AJ, Liang GZ, Yuan L (2010) Compos Part A 41:1321
41. Burnside SD, Giannelis EP (2000) J Polym Sci B 38:1595